Multiobjective Optimal Design of a Voltage Supply Inverter Fed In-Wheel Synchronous Motor

C. Versèle[1], *Student Member*, *IEEE*, O. Deblecker[1], *Member*, *IEEE*,
Z. De Grève[1,2], *Student Member*, *IEEE*, and J. Lobry[1], *Member*, *IEEE*

[1] UMons, Faculté Polytechnique de Mons, Electrical Engineering Department, Bd Dolez 31, B-7000 Mons, Belgium
[2] F.R.S/FNRS, Fonds de la Recherche Scientifique, Rue d'Egmont 5, B-1000 Bruxelles

Christophe.Versele@umons.ac.be

***Abstract*-This paper deals with the multiobjective optimal design of a voltage supply inverter (VSI) fed in-wheel motor for urban electric vehicles (EVs) using genetic algorithms (GAs). The proposed motor is an axial flux permanent magnet (AFPM) synchronous sine-wave motor. This type of motor can be directly integrated into the wheel without mechanical transmission and differential gears. The design problem requires minimizing the weights and the losses of the motor and the VSI. The simultaneous optimization of the in-wheel motor and its own VSI results in a system optimized towards the requirements of the EV.**

***Keywords*-Multiobjective design optimization; genetic algorithms; electric vehicle; axial flux permanent magnet synchronous motor.**

I. INTRODUCTION

Battery EVs and hybrid EVs are now at the forefront of transportation researches in order to reduce the emission of pollutant gasses, especially in the inner cities. However, the present performances of EVs are far from being competitive to those of traditional internal combustion engine vehicles, mainly in terms of autonomy. Therefore, power-saving and mass-saving are of the upmost importance when designing the entire drive system of EVs and, particularly, their electric motor drives [1].

In conventional EVs, the power system consists of battery, electric motors with drives, transmission gears and differentials to the wheels [2]. The mechanical transmission system contributes greatly to the power loss, through the heat dissipation in the various components, and to the weight of the vehicle. An interesting alternative to this conventional power system is the concept of in-wheel motors or hub-in motors as illustrated in Fig. 1. In this concept, the motor is directly integrated into the wheel, thus eliminating transmission gears and differentials with their associated power loss [3]. Furthermore, the elimination of mechanical components in transmission chains or gears reduces the weight of the vehicle. Each of the in-wheel motors has its own VSI as well as its own speed or torque controller. All the in-wheel motors are coordinated by a digital vehicular-speed controller with differential gear [1].

Due to their robustness, low cost, performances and simplicity of design, induction motors (IMs) are often preferred for EVs propulsion. However, in recent years, Neodymium-Iron-Bore (NdFeB) AFPM motors have become an interesting alternative to IMs due to their compactness, low weight and high torque density. Moreover, AFPM motors are pancake-type, fit perfectly the wheel of an automobile vehicle and, thus, can be easily and compactly integrated into the wheel. According to these properties, axial flux motor seems to be a better choice than more conventional radial flux motor for this kind of application.

There are many alternatives for the design of AFPM motors [4]: slotted or slotless stator, rotor with interior or surface-mounted permanent magnets (PMs), internal or external rotor, number of rotors, number of stators, etc. In this paper, a double-sided motor with internal slotted stator and surface-mounted PMs is proposed as basic design choice essentially motivated by the presence of two air gaps doubling the torque.

Among the various researches, many authors have published papers about the optimal design of in-wheel motors for EVs or wheelchairs [1], [2], [3], [5], [6] as well as about the optimization of AFPM motors [7], [8], [9].

In this paper, the objective is to optimize simultaneously one of the four in-wheel motors of an EV and its own VSI in terms of weight and power loss. Note that the simultaneous optimization of the in-wheel motor and its own VSI, rarely discussed in literature, results in a system optimized towards the requirements of the EV. This is an advantage of the design procedure proposed in this paper.

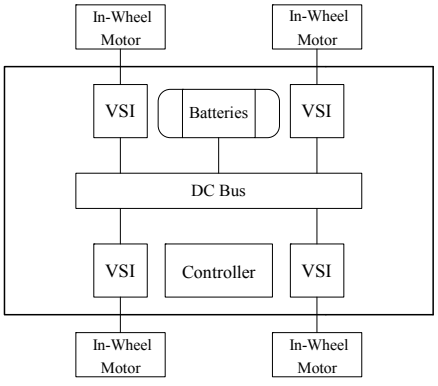

Figure 1. In-wheel motors drive

978-1-4244-8218-4/10/$26.00 ©2010 IEEE

To do so, a multiobjective optimization (MO) technique based on evolutionary algorithms (EAs) is used. EAs are stochastic search techniques that mimic natural evolutionary principles to perform search and optimization procedure [10]. Among the several approaches to evolutionary optimization, GAs have been chosen and the so-called Elitist Nondominated Sorting Genetic Algorithm (NSGA-II) [10] is used to perform the optimal design of the in-wheel motor and its own VSI. Note that GAs are chosen because they have already proved their efficiency to optimize every kind of electrical machines [11] and power electronics converters [12], [13].

The remainder of this paper is organized as follows. First, the requirements in terms of power and torque of an EV are discussed in Section II. Then, Section III describes the AFPM motors and VSI models used in the design procedure. In Section IV, the MO technique based on GAs as well as the proposed optimization routine are described. Finally, in Section V, a design example is presented and the advantages of the new design procedure are discussed in Section VI.

II. Requirements Of An EV

In order to determine the requirements, in terms of power and torque, of one of the four in-wheel motors (considering an EV driven by four in-wheel motors), a computer model of an EV traction system is presented in this section.

The road load on the vehicle consists of three forces [2]: (1) the rolling resistance F_r, (2) the aerodynamic drag force F_a and (3) the climbing force F_c which are expressed as [14]:

$$F_r = f_r \cdot M_v \cdot g \tag{1}$$

$$F_a = 0.5 \cdot \rho \cdot A_f \cdot C_D \cdot \left(v + v_w\right)^2 \tag{2}$$

$$F_c = M_v \cdot g \cdot \sin\left(\alpha\right) \tag{3}$$

where f_r is the rolling resistance coefficient (which is an empirical coefficient depending on the road-tire friction), M_v is the mass of the vehicle, g is the earth gravity acceleration, ρ is the air density, A_f is the frontal area of the vehicle, C_D is the coefficient of aerodynamic resistance (that characterizes the shape of the vehicle), v is the vehicle speed, v_w is the component of the wind speed on the vehicle's moving direction and α is the road angle (deduced from the road slope). According to Newton's second law, the total tractive effort F_t required to reach the desired acceleration a and to overcome the road load is:

$$F_t = M_v \cdot a + F_r + F_a + F_c . \tag{4}$$

Once the total tractive effort is computed, the total torque T_t and power P_t required to be produced by the four in-wheel motors can be expressed as:

$$T_t = F_t \cdot r_{wheel} \tag{5}$$

$$P_t = T_t \cdot \Omega_{wheel} \tag{6}$$

where r_{wheel} is the drive wheels radius and Ω_{wheel} is the rotational wheels speed.

Based on the specifications of an urban EV [14], summarized in Table I, and on the above-described EV traction system, the requirements of one in-wheel motor can be easily computed. All the results are presented in Table II. Note that, in addition to provide its requirements, the in-wheel motor must also respect some constraints. The main constraints are the total weight of each of the four in-wheel motors M_{motor} (imposed by the maximal authorized "unsprung" wheel weight) and the imposed outer radius R_{out} of the motor (imposed by the rim of the wheel). Those are also specified in Table I and Table II.

III. Modeling Of The AFPM Motor And VSI

In order to evaluate the two objective functions, viz. the weight and the losses of the motor and the VSI, and to verify if the constraints are not violated during the design procedure, two models are necessary: one for the motor and one for the VSI. It should be noticed that analytical models have been chosen in this paper with the aim of reducing the computational time. These models must permit to evaluate the weight and the losses of the motor and the VSI as well as to estimate the torque and power developed by the motor.

A. AFPM motor model

Analytical design of AFPM motor is usually performed on the average radius of the machine [15] that allows evaluating motor parameters and performances based on analytical design methods explained in details in literature [16]. Therefore, only the fundamental analytical design equations are addressed below for conciseness. Moreover, the analytical model used in this paper has been detailed and validated by experimental results elsewhere [17].

Using the remanence flux density B_r and the relative permeability μ_{ra} of the PMs as well as the geometrical dimensions of the air gap and the PMs (thickness and area), the air gap flux density B_g is calculated according to:

$$B_g = k_{\sigma PM} \cdot B_r \Big/ \left(1 + \mu_{ra} \cdot k_C \cdot g \Big/ l_{PM} \cdot S_{PM} \Big/ S_g\right) \tag{7}$$

where g and l_{PM} are respectively the air gap thickness and PM thickness (see Fig. 2); S_g and S_{PM} are respectively the air gap area and PM area. In (7), $k_{\sigma PM}$ (<1) is a factor that takes into account the leakage flux and k_C (>1) is the Carter coefficient.

TABLE I.
SPECIFICATIONS OF AN EV

Weight M_v	1150 kg
Max. speed v_{max}	13.9 m/s (50 km/h)
Acceleration a	1 m/s²
Frontal area A_f	2.5 m²
Coefficient of aerodynamic resistance C_D	0.32
Rolling resistance coefficient f_r	0.015
Max. road angle α	5.7° (10%)
Rim diameter	14''
Number of in-wheel motors	4

TABLE II.
REQUIREMENTS OF ONE IN-WHEEL MOTOR

Torque T_t	> 107 Nm
Power P_t	> 8.7 kW
Weight of the motor M_{motor}	< 43.125 kg

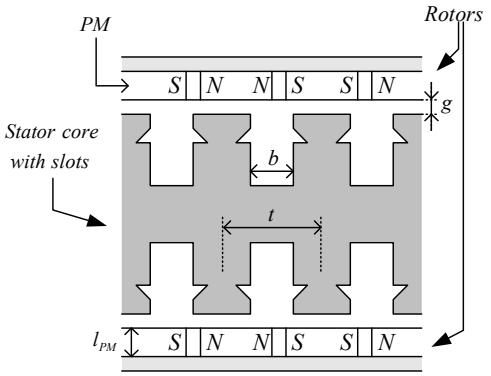

Figure 2. Double-sided AFPM motor with internal slotted stator

On the one hand, the main magnetic flux density in the air gap decreases under each slot opening due to the increase in the reluctance. The Carter coefficient permits to take into account this change in magnetic flux density caused by slot openings defining a fictitious air gap greater than the physical one. It can be computed as follows [16]:

$$k_C = \frac{t}{t - \gamma \cdot g} \tag{8}$$

where t is the average slot pitch (see Fig. 2) and γ is a coefficient defined by [16]:

$$\gamma = \frac{4}{\pi} \cdot \left[\frac{b}{2 \cdot g} \cdot \arctan\left(\frac{b}{2 \cdot g} \right) - \ln \sqrt{1 + \left(\frac{b}{2 \cdot g} \right)^2} \right] \tag{9}$$

where b is the width of slot opening.

On the other hand, in order to obtain an accurate estimation of the air gap flux density and the torque developed by the motor, the factor $k_{\sigma PM}$ is one of the most essential quantities that must be computed. Indeed, the leakage flux has a substantial effect on the flux density within the air gap and PMs [18] and, therefore, on the torque developed by the motor (see (10)). In addition to air gap leakage flux, zigzag leakage flux is another main part of the leakage flux. The zigzag leakage flux is the sum of three portions [18]: the first part of the zigzag leakage flux is short-circuited by one stator tooth, the second part links only part of the windings of a phase, and, the third part travelling from tooth to tooth does not link any coil. Note that, in this paper, an analytical model developed by Qu and Lipo [18] for the purpose of the design of surface-mounted PM machines is used to compute the factor $k_{\sigma PM}$. This model permits to express this factor in terms of the magnetic material properties and dimensions of the machine. It is thus very useful during the design stage.

Assuming sinusoidal waveform for the air gap flux density and phase current, the average electromagnetic torque T of a double-sided AFPM motor can be calculated by [16]:

$$T = 2 \cdot \pi \cdot B_g \cdot A_{in} \cdot R_{out}^3 \cdot k_d \cdot \left(1 - k_d^2\right) \tag{10}$$

where A_{in} is the linear current density on the inner radius of the machine and k_d is the ratio between inner and outer radii of the rotor disk. It should be noticed that, for a given outer radius and magnetic and electric loadings, the factor k_d is very important to determine the maximum torque developed by the motor [9]. So, this factor will be one of the optimization variables.

The double-sided AFPM motor losses are the sum of the stator winding losses, the stator and rotor cores losses and the PMs losses, whereas its weight is the sum of the stator and the two rotors weights, the stator winding weight and the PMs weight. Note that the computation of those different parts of the two objective functions can easily be found elsewhere [16] and, so, it is not described in this paper.

B. VSI model

The total loss of the semiconductor devices (IGBTs and diodes) of the VSI (employing sinusoidal pulse-width-modulation) consists of two parts: the on-state losses and the switching losses. The on-state losses of the devices are calculated from their average I_{ave} and rms I_{rms} currents by the well-known expression [19]:

$$P_{on} = V_{th} \cdot I_{ave} + r \cdot I_{rms}^2 \tag{11}$$

where V_{th} represents the threshold voltage and r the on-state resistance, both taken from the manufacturer's data sheets.

The switching losses are, as for them, calculated by the following formula [19]:

$$P_{sw} = f_s \cdot \left(E_{turn-on} + E_{turn-off} \right)_{T_j, I_C, V_{CE}} \tag{12}$$

where $E_{turn\text{-on}}$ and $E_{turn\text{-off}}$ are the energies dissipated during the transitions, both taken from the manufacturer's data sheets, at given junction temperature T_j, on-state collector current I_C and blocking voltage V_{CE}. Note that the average and rms values of the current used in (11) can easily be computed assuming sinusoidal current waveforms.

Based on the total loss of the semiconductor devices, the heatsink can be designed in order to limit the junction temperature to a predefined temperature (typically in the order of 125 °C). This temperature can be estimated from the ambient temperature T_a, the thermal resistances (junction-case: $R_{th,jc}$, case-heatsink: $R_{th,ch}$ and heatsink-ambient: $R_{th,ha}$) and the total loss P_{sc} of all the semiconductor devices by:

$$T_j = T_a + \left(R_{th,jc} + R_{th,ch} + R_{th,ha} \right) \cdot P_{sc} . \tag{13}$$

From (13), the thermal resistance of the heatsink $R_{th,ha}$ needed to limit the junction temperature to the predefined value can be computed and, then, the heatsink can be selected from manufacturer's data sheets.

The total weight of the VSI is the sum of the weight of all the semiconductor devices and the weight of the heatsink.

IV. Optimization Routine Based On NSGA-II

As mentioned previously, in this contribution, a multiobjective optimization technique based on EAs is used. Those are stochastic search techniques that mimic natural evolutionary principles to perform the search and optimization procedures [10]. Among the several approaches to evolutionary optimization, GAs have been chosen and the so-called NSGA-II [10] is used to perform the design. It should be noticed that the presence of several conflicting

objectives in a problem gives rise to a set of optimal solutions (known as Pareto-optimal solutions) instead of a single optimal solution. This set of Pareto-optimal solutions constitutes the Pareto front.

A. NSGA-II

NSGA-II is a recent and efficient multiobjective EA using an elitist approach [10]. It relies on two main notions: nondominated ranking and crowding distance. Nondominated ranking is a way to sort individuals in nondominated fronts whereas crowding distance is a parameter that permits to preserve diversity among solutions of the same nondominated front.

The procedure of the *NSGA-II* is shown in Fig. 3 and is as follows [10]. First, a combined population R_t (of size $2 \cdot N$) of the parent P_t and offsprings Q_t populations (each of size N) is formed. Then, the population R_t is sorted in nondominated fronts. Now, the solutions belonging to the best nondominated set, i.e. F_1, are of best solutions in the combined population and must be emphasized more than any other solution. If the size of F_1 is smaller than N, all members of F_1 are inserted in the new population P_{t+1}. Then, the remaining population of P_{t+1} is chosen from subsequent nondominated fronts in order of their ranking. Thus, the solutions of F_2 are chosen next, followed by solutions from F_3. However, as shown in Fig. 3, not all the solutions from F_3 can be inserted in population P_{t+1}. Indeed, the number of empty slots of P_{t+1} is smaller than the number of solutions belonging to F_3. In order to choose which ones will be selected, these solutions are sorted according to their crowding distance (in descending order) and, then, the number of best of them needed to fill the empty slots of P_{t+1} are inserted in this new population. The created population P_{t+1} is then used for selection, crossover and mutation (see below) to create a new population Q_{t+1}, and so on for the next generations.

NSGA-II has been implemented in Matlab with real and binary coding schemes. So, a discrete variable is coded in a binary string whereas a continuous variable is coded directly. Such coding schemes are used in this paper because the considered optimization variables (see Table III in Section V) belong to the two categories.

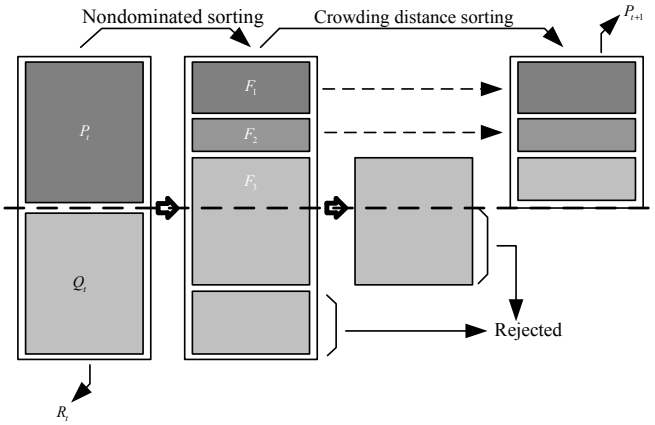

Figure 3. *NSGA-II* procedure [10]

These coding schemes allow a natural way to code different optimization variables, which is not possible with traditional optimization methods. Moreover, the real coded scheme for the continuous variables eliminates the difficulties (Hamming cliff problem and difficulty to achieve arbitrary precision) of coding such variables with a binary scheme [20].

So, e.g., with the coding scheme used in this paper, the structure of the chromosome (composed by the seven considered optimization variables) of the solution #3 (see Table IV in Section V) is as follows:

$$\underbrace{(k_d)(J)(l_{PM})(g)(f_s)}_{\text{real coded variables}}\ \underbrace{(p)(q)}_{\text{binary coded variables}}$$

$$\downarrow$$

$$(0.89)(5.9)(5)(1)(1.5)\underbrace{(1011)}_{\rightarrow 11}\underbrace{(10010110)}_{\rightarrow 150}$$

There are three fundamental operations used in GAs: selection, crossover and mutation. The primary objective of the selection operator is to make duplicate of good solutions and eliminate bad solutions in a population, in keeping the population size constant. To do so, a tournament selection [10] based on nondominated rank and crowding distance of each individual is used. Then, the selected individuals generate offsprings from crossover and mutation operators. To cross and to mutate the real coded variables the Simulated Binary Crossover and Polynomial Mutation operators [20] are used in this paper. The single-point crossover [20] is, as for it, used to cross the discrete optimization variables. Note that to mutate this type of variables, a random bit of their string is simply changed from '1' to '0' or *vice versa*.

Finally, the constraints must be taken into account. Several ways exist to handle constraints in EAs. The easiest way to take them into account in *NSGA-II* is to replace the non-dominated ranking procedure by a constrained non-dominated ranking procedure as suggested by its authors elsewhere (see, e.g., [10]). The effect of using this constrained-domination principle is that any feasible solution has a better nondominated rank than any infeasible solution.

It is important to emphasize that the GA must be properly configured. The size of the population is one of the important parameters of the GA as well as the termination criterion. In this contribution, the size of the population N_{pop} is taken equal to 100. It is important to note that, on the one hand, N_{pop} should be large enough to find out small details of the Pareto front whereas, on the other hand, N_{pop} should not be too large to avoid long time optimization. The termination criterion consists in a pre-defined number of generations which is here also arbitrarily fixed to 400. Finally, the crossover probability and the mutation probability are respectively chosen to be 0.85 and 0.015 as typically suggested in literature [10].

B. Design procedure

The overall design procedure, presented in Fig. 4, has been implemented in the Matlab environment. First, a random initial population is generated. Then, the objective functions,

i.e. the total weight and the total losses of the VSI-fed AFPM in-wheel motor, are evaluated based on the initial population and on the above-described models (see Section III). A convergence test is then performed to check for a termination criterion. If this criterion is not satisfied, the reproduction process using genetic operations starts. A new population is generated and the previous steps are repeated until the termination criterion is satisfied. Otherwise, the Pareto front, i.e. the nondominated solutions within the entire search space, is plotted and the optimization procedure ends.

V. Design Example

In order to illustrate the design procedure, a VSI-fed AFPM in-wheel motor with the specifications given in Tables I and II is designed.

The lower and upper bounds of the seven considered optimization variables, viz. the factor k_d, the current density in the conductors J, the air gap thickness g, the PMs thickness l_{PM}, the number of poles pairs p, the number of slots q and the switching frequency f_s, are specified in Table III. Note that the variables p and q are discrete ones whereas the others are continuous ones.

It should also be recalled that the in-wheel motor must provide the requirements of the EV as well as respecting some constraints. The main constraints are the total weight M_{motor} of each of the four in-wheel motor and the imposed outer radius of the motor R_{out}. Note that these constraints have already been specified in Tables I and II.

The results, i.e. the Pareto front, are presented in Fig. 5. Each point of this Pareto front represents an optimal VSI-fed AFPMS in-wheel motor that respects all the constraints. Moreover, the values of the optimization variables corresponding to three particular solutions of this front are also detailed in Table IV. Note that the solution #3 corresponds to a good trade-off between the two objective functions.

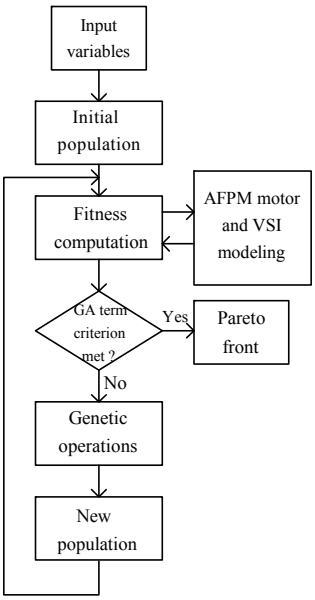

Figure 4. Flowchart of the design procedure using GAs

TABLE III.
OPTIMIZATION VARIABLES

Variables	Bounds	Type
k_d	[0.5 ; 0.9]	Continuous
J	[1 ; 6] A/mm²	Continuous
l_{PM}	[1 ; 20] mm	Continuous
g	[1 ; 5] mm	Continuous
f_s	[1 ; 10] kHz	Continuous
p	[1 ; 12]	Discrete
q	[50 ; 150]	Discrete

Considering (10), one can easily conclude that the maximum value of the torque is reached for a value of k_d equal to 0.58. However, the optimal value of this factor found by the optimization procedure is around 0.85 to 0.9 (see Table IV). This result is not surprising because it has been shown elsewhere [9] that the maximum value of the torque to weight ratio is obtained for values around 0.85 and, here, the weight must be minimized.

From Table IV, one can also conclude that the variables l_{PM}, g, f_s, p and q have converged to optimal values and that all solutions respect all the requirements of the EV (in terms of minimum torque and power) as well as the motor weight constraint (see Tables II and IV).

VI. Advantages Of The Design Procedure

The design procedure proposed in this paper presents several advantages.

A first advantage of this design procedure is that it is multiobjective. So, several conflicting objectives, often present in engineering design problems, can be optimized simultaneously.

A second advantage is the number of solutions considered in a small time. Indeed, the optimization procedure compares a large number of solutions (in the order of several thousands) to retain only the best in a time in the order of 180 s (for 400 generations of 100 individuals with a Pentium (R) D CPU 3.40 GHz, 3 Go RAM).

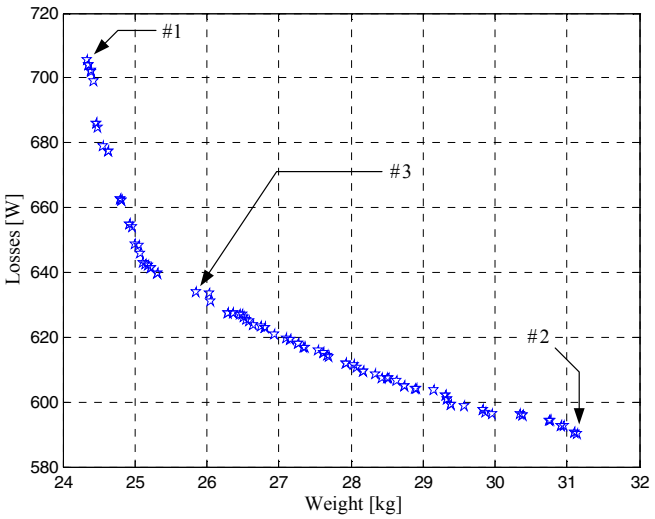

Figure 5. Pareto front

TABLE IV.
DETAILS OF THREE PARTICULAR SOLUTIONS

	#1	**#2**	**#3**
k_d	0.89	0.87	0.89
J [A/mm²]	6.8	4.8	5.9
l_{PM} [mm]	5.3	5	5
g [mm]	1.8	1	1
f_s [kHz]	1.7	1.4	1.5
p	12	10	11
q	150	150	150
T_t [Nm]	207	207	207
P_t [kW]	8.719	8.720	8.724
M_{Motor} [kg]	19.8	27.6	21.9

A third advantage is the simultaneous optimization of the in-wheel motor and its own VSI. Indeed, it results in a system optimized towards the requirements of the EV.

Finally, the design procedure has the major advantage that a set of optimal solutions – instead of a single one – is proposed to the designer who can choose *a posteriori* which objective function to promote and, then, select a particular VSI-fed in-wheel motor. So, a degree of freedom is still available at the end of the optimization procedure and, moreover, in industrial framework, this set of solutions can be confronted with additional criteria or engineer know-how not included in models.

VII. CONCLUSION

This paper has addressed the problem of MO design of a VSI-fed AFPM synchronous motor using GAs and a new design procedure has been proposed. The weight and the losses of the motor and the VSI have been chosen as objective functions whereas the factor k_d, the current density in the conductors, the air gap thickness, the PMs thickness, the number of poles pairs, the number of slots and the switching frequency have been chosen as optimization variables. Finally, the design procedure has been illustrated by the design of a VSI-fed AFPM in-wheel motor for an urban EV.

REFERENCES

[1] K.-J. Tseng and G. H. Chen, "Computer-Aided Design and Analysis of Direct-Driven Wheel Motor Drive", *IEEE Trans. Power Electron.*, vol. 12, no. 3, pp. 517-527, May 1997.

[2] Y.-P. Yang and D. S. Chuang, "Optimal Design and Control of a Wheel Motor for Electric Passengers Cars", *IEEE Trans. Magn.*, vol. 43, no. 1, pp. 51-61, Jan. 2007.

[3] Y.-P. Yang, Y.-P. Luh and C.-H. Cheung, "Design and Control of Axial-Flux Brushless DC Wheel Motors for Electric Vehicles – Part I: Multiobjective Optimal Design and Analysis", *IEEE Trans. Magn.*, vol. 40, no. 4, pp.1873-1882, July 2004.

[4] F. Sahin and A. J. A. Vandenput, "Design Considerations of the Flywheel-Mounted Axial-Flux Permanent Magnet Machine for a Hybrid Electric Vehicle", in *8th Power Electronics and Application Conf. Proc.*, EPE 1999, Lausanne, Sept. 1999.

[5] C. Espanet, J. M. Kauffmann, F. Wurtz and J. Bigeon, "Application of a new optimization approach to the design of electrical wheels", *IEEE Trans. Energy Conversion*, vol. 14, no. 4, pp.952-958, Dec. 1999.

[6] R. Nilssen, S. E. Skaar, R. Lund, T. Skjellnes, S.Øvrebø and E. Løvli, "Design of a permanent magnet synchronous integrated in the wheel rim on wheelchairs", in *11th Power Electronics and Application Conf. Proc.*, EPE 2005, Dresden, Sept. 2005.

[7] Y.-D. Chun, D.-H. Koo and Y.-H. Cho, "Multiobjective optimization design of axial flux permanent magnet motor", *International Journal of Applied Electromagnetics and Mechanics*, vol. 25, no. 1, pp. 613-619, IOS Press, 2007.

[8] G. Cvetkovski and L. Petkovska, "Efficiency Maximisation in Structural Design Optimisation of Permanent Magnet Synchronous Motor", in 18th *Int. Conf. Eletric. Machines Proc.*, ICEM 2008, Vilamoura, Sept. 2008.

[9] J. Azzouzi, R. Belfkira, N. Abdel-Karim, G. Barakat and B. Dakyo, "Design Optimization of an Axial Flux PM Synchronous Machine: Comparison Between DIRECT Method and GAs Method", in *12th Int. Power Electronics and Motion Control Conf. Proc.*, EPE-PEMC 2006, Portoroz, Sept. 2006.

[10] K. Deb, "Multi-Objective Optimization using Evolutionary Algorithms", John Wiley & Sons, Inc., New Jersey, 2002.

[11] S. E. Skaar and R. Nielssen, "Genetic Optimization of Electric Machines, a State of the Art Study", in *10th Power Electronics and Application Conf. Proc.*, EPE 2003, Toulouse, Sept. 2003.

[12] D. V. Malyna, J. L. Duarte, M. A. M. Hendrix and F. B. M. van Horck, "Optimization of Combined Thermal and Electrical Behavior of Power Converters Using Multi-Objective Genetic Algorithms", in *12th Power Electronics and Application Conf. Proc.*, EPE 2007, Aalborg, Sept. 2007.

[13] H. Helali *et al.*, "Power converter's optimisation and design. Discrete cost function with genetic based algorithms", in *11th Power Electronics and Application Conf. Proc.*, EPE 2005, Dresden, Sept. 2005.

[14] M. Ehsani, Y. Gao and S. E. Gay, "Modern Electric, Hybrid Electric and Fuel Cell Vehicles: Fundamentals Theory, and Design", CRC Press, 2005.

[15] A. Parviainen, M. Niemelä and J. Pyrhönen, "Analytical, 2D FEM and 3D FEM Modelling of PM Axial Flux Machine", *in 10th Power Electronics and Application Conf. Proc.*, EPE 2003, Toulouse, Sept. 2003.

[16] J. F. Gieras, R.-J. Wang and M. J. Kamper, "Axial Flux Permanent Magnet Brushless Machines", Kluwer Academic Publishers, Netherlands, 2004.

[17] C. Versèle *et al.*,, "Analytical Design of an Axial Flux Permanent Magnet In-Wheel Synchronous Motor for Electric Vehicle", in *13th Power Electronics and Application Conf. Proc.*, EPE 2009, Barcelona, Sept. 2009.

[18] R. Qu and T. A. Lipo, "Analysis and Modeling of Airgap & Zigzag Leakage Fluxes in a Surface-Mounted-PM Machine", *Records of the 37th Industry Applications Conf.*, IAS 2002, Penssylvania, October 2002.

[19] O. Deblecker, A. Moretti and F. Vallée, "Comparative Study of Soft-Switched Isolated DC-DC Converters for Auxiliary Railway Supply", *IEEE Trans. Power Electron.*, vol. 23, no. 5, pp. 2218-2229, Sept. 2008.

[20] K. Deb and M. Goyal, "Optimization Engineering Designs Using a Combined Search", in *7th Int. Conf. on Genetic Algorithms Proc.*, 1997.